UWB Slot Antenna with Band-Notched Property with Time Domain Modeling based on Genetic Algorithm Optimization

Javad Zolghadr[1], Yuanli Cai[1], and Nasser Ojaroudi[2]

[1] School of Electronic and Information Engineering, Xi'an Jiaotong University, Xi'an 710049, China
Javad.zolghadr@gmail.com, ylicai@mail.xjtu.edu.cn

[2] Young Researchers and Elite Club, Ardabil Branch, Islamic Azad University, Ardabil, Iran
n.ojaroudi@yahoo.com

Abstract ─ This paper presents a kind of band-notched slot antenna with time domain designing method for ultra-wideband (UWB) applications. The proposed antenna consists of a square radiating stub with a defected mircostrip feed-line using an M-shaped step impedance resonator (SIR) slot and a defected ground plane with a pair of inverted U-shaped slots. By cutting two inverted U-shaped slots in the ground plane, a new resonance at the higher frequencies is excited and hence much wider impedance bandwidth can be produced that. To generate a band-notched characteristic, we use an M-shaped slot at the feed-line. The proposed antenna can operate from 3.03 to 13.21 GHz with frequency band-notched function in 7.28-7.79 GHz to avoid interference from downlink of X-band satellite communication systems. To verify the validation of the proposed antenna an equivalent circuit based on time domain reflectometry (TDR) analysis is presented. In addition, the accuracy of the equivalent circuit models have been improved using Genetic algorithm optimization (GAP). Detailed simulation and numerical investigations are conducted to understand their behaviors and optimize for broadband operation. The proposed antenna exhibits almost omni-directional radiation patterns in UWB frequency range and could be used in wireless systems.

Index Terms ─ Band-notched function, GAP, microstrip-fed slot antenna, TDR analysis, UWB systems.

I. INTRODUCTION

In UWB communication systems, one of key issues is a design of compact antennas while providing wideband characteristic over the whole operating band [1]. Consequently, a number of planar antennas with different geometries have been experimentally characterized [2-5] and automatic design methods have been developed to achieve the optimum planar shape. Moreover, other strategies to improve the impedance bandwidth have been investigated [6-8]. The frequency range for UWB systems between 3.1–10.6 GHz will cause interference to the existing wireless systems for example the wireless local area network (WLAN) for IEEE 802.11a operating in 5.15–5.35 GHz and 5.725–5.825 GHz bands or 7.25-7.75 GHz for downlink of X-band satellite systems, so the UWB antenna with a band-notched function is required [9-15].

In this paper, a simple method for designing a novel and compact microstrip-fed slot antenna with band-stop performance and time domain reflectometry analysis for UWB applications has been presented. In the proposed antenna for bandwidth enhancement, based on defected ground structures (DGS) we use a pair of inverted U-shaped slots in the ground plane and also based on defected microstrip structures (DMS) theory, to generate a band-stop performance an M-shaped slot was inserted at feed-line [16]. Unlike other band-notched UWB antennas reported in the literature to date, this structure has an ordinary square radiating stub configuration. We also report their circuit models based on TDR analysis. The proposed band-notched UWB antenna has a compact size. Good VSWR and radiation pattern characteristics are obtained in the frequency band of interest. Simulated and measured results are presented to validate the usefulness of the proposed microstrip-fed slot antenna structure for UWB applications.

II. ANTENNA DESIGN

The presented slot antenna fed by a 50 Ω microstrip line is shown in Fig. 1, which is printed on an FR4 substrate of width W_{sub}=20 mm and length $L_{sub} = 20 mm$, thickness 0.8 mm, permittivity 4.4, and loss tangent 0.018. The basic antenna structure consists of a square radiating stub, a feed line, and a ground plane. The radiating stub is connected to a feed line of width W_f=1.5 mm and length L_f=5 mm. The equivalent circuit model of the proposed design is illustrated in Fig. 2. The antenna is designed to work at the frequency range of from 3.03 to 13.21 GHz.
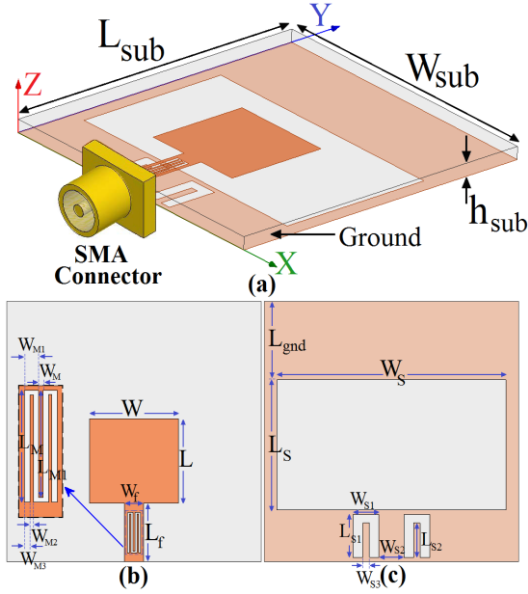
Fig. 1. Geometry of the proposed slot antenna: (a) side view, (b) top layer, and (c) bottom layer.
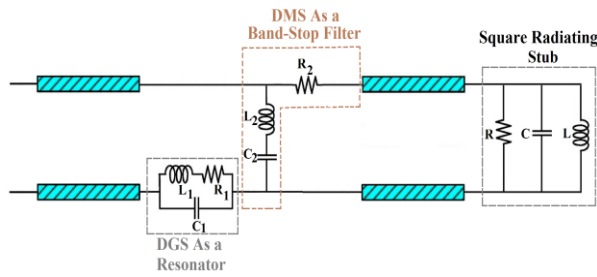

Fig. 2. The proposed antenna equivalent circuit model.

The proposed antenna is connected to a 50 Ω SMA connector for signal transmission. The final dimensions of the designed antenna are as follows:

$W_{sub} = 20\,mm$, $L_{sub} = 20\,mm$, $h_{sub} = 0.8\,mm$, $W = 7\,mm$,

$L = 7\,mm$, $W_f = 1.5\,mm$, $L_f = 5\,mm$, $W_S = 18\,mm$,

$L_S = 10\,mm$, $W_{S1} = 2\,mm$, $L_{S1} = 4.7\,mm$, $W_{S2} = 2\,mm$,

$L_{S2} = 2.85\,mm$, $W_{S3} = 0.5\,mm$, $L_M = 3.7\,mm$,

$W_M = 0.2\,mm$, $L_{M1} = 3.6\,mm$, $W_{M1} = 0.5\,mm$,

$W_{M2} = 0.15\,mm$, and $L_{gnd} = 6\,mm$.

A. Defected structures (DGS and DMS) and these equivalent circuit models

Recently, defected ground plane structures (DGS) and defected microstrip structure (DMS) have been proposed for suppression of spurious response in the microstrip structures [17-18]. These configurations provide the band-stop characteristics.

The proposed DGS and DMS with their equivalent

circuit models are shown in Fig. 3, which is printed on a FR4 substrate of thickness 0.8 mm, permittivity 4.4, and loss tangent 0.018. The corresponding geometrical parameters of the proposed structures are denoted in Fig. 3. This defected ground structures on the ground plane and feed-line will perturb the incident and return current and induce a voltage difference on the ground plane and microstrip feed-line. The proposed DGS can be modeled as a resonator with parallel LC circuit [19]. The resistance in equivalent circuits represents the loss of the slot and slit, which is small in general [20]. The proposed DMS act as a band-stop filter therefore can be modeled with series and parallel LC circuit.
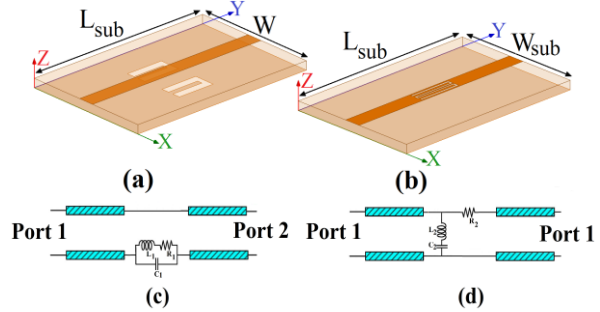

Fig. 3. The proposed defected structures, (a) DGS and (b) DMS with their equivalent circuit models in (c) and (d).

B. Time domain reflectometry analysis

In this section, the proposed defected structures with mentioned design parameters were simulated, and the TDR results of the input impedance for them in equivalent circuit and full-wave analysis cases are presented and discussed. The simulated full-wave TDR results are obtained using the Ansoft simulation software high-frequency structure simulator (HFSS) [21].

Figures 4 and 5 show the simulated reflection waveform observed at Port1 of the defected structures, as shown in Fig. 3 (a) and Fig. 3 (b), and with a 50 termination on Port2. The excitation source is a step wave with amplitude 1Volt and rise time of 30psec. The corresponding result predicted by the equivalent circuit model is also shown in these figures. As shown in Figs. 4 and 5, TDR curves have started with impedance just under 50 Ω. This is indeed the characteristic impedance of the microstrip line. At impedance discontinuities, part of the input signal is reflected. These reflections, after traveling back, reach terminal Port1 and are observed there [12]. From these observations, the characteristic impedances along the transmission line can be computed. The optimal dimensions of the equivalent circuit models parameters are specified in Table 1.
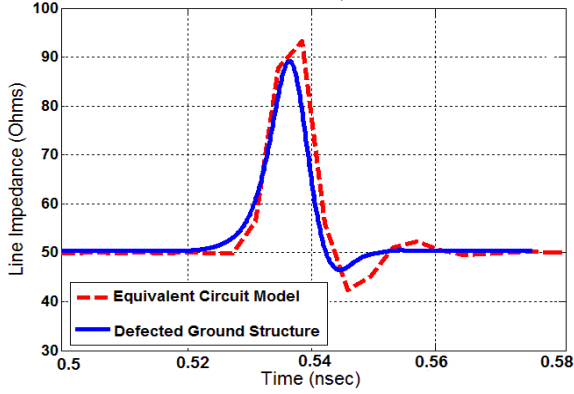
Fig. 4. The reflected waveforms simulated by HFSS and predicted by equivalent circuit model of the proposed defected ground structure.
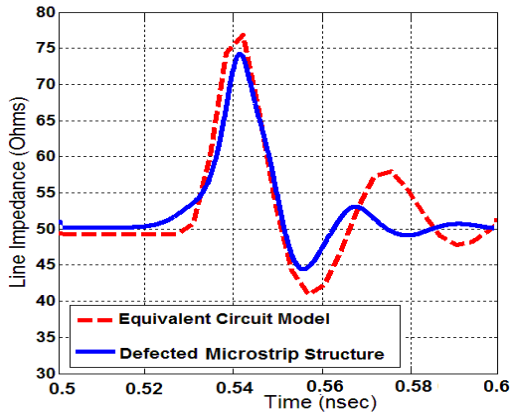

Fig. 5. The reflected waveforms simulated by HFSS and predicted by equivalent circuit model of the proposed defected microstrip structure.

Table 1: Equivalent circuit model parameters

Element	Value	Element	Value
L1	1.55 (nH)	L2	4.8 (nH)
C1	1.05 (pF)	C2	1.75 (pF)
R1	0.8 (Ω)	R2	2.1 (Ω)

C. TDR and genetic algorithm analysis

In order to calculate of the TDR results for the proposed equivalent circuits, we can write the reflection coefficient through defected structures as (1) which is observed at the source end, i.e., Port1:

$$\Gamma_Z(s) = \frac{Z(s)}{Z(s)+2Z_0}. \tag{1}$$

A step voltage source with rise time τ_r and amplitude V_0, can be expressed [15-16] as:

$$V_{in}(s) = \frac{V_0}{2\tau_r}\frac{1}{s^2}\left(1-e^{-\tau_r S}\right). \tag{2}$$

Therefore, the reflected waveform in Laplace domain can be written as:

$$V_{TDR}(s) = V_{in}(s)\Gamma_{DGS,DMS}(s). \tag{3}$$

In TDR measurements, the impedance follows from:

$$Z_{TDR} = Z_0 \times (V_{in}(t)+V_{TDR}(t))/(V_{in}(t)-V_{TDR}(t)), \tag{4}$$

where Z_0 is the characteristic impedance of the transmission line at the terminal.

In order to optimize TDR result with genetic algorithm results for the equivalent circuits, the impedance of these circuits in Laplace domain can be represented as follows:

$$z_{11} = \frac{V_1}{I_1}\Big|_{I_2=0} = \tag{5}$$
$$\left[\left(R_2+\frac{1}{C_2+S}+L_2S\right)\Big\|(L_3S\Big\|\frac{1}{C_3S})+\frac{1}{C_1S}+L_1S\right]\|R_1$$

$$\begin{cases} Z=(R_1+L_1S+\frac{1}{C_1S})\Big\|(L_3S\Big\|\frac{1}{C_3S})+L_2S+\frac{1}{C_2S} \\ \\ Z_{12}=\frac{V_1}{I_2}\Big|_{I_1=0}=R_1\times\frac{R_2}{R_2+Z}\times\dfrac{L_3S\Big\|\frac{1}{C_3S}}{L_3S\Big\|\frac{1}{C_3S}+\frac{1}{C_1S}+L_1S+R_1} \end{cases} \tag{6}$$

$$\begin{cases} Y=(R_2+L_2S+\frac{1}{C_2S})\Big\|(L_3S\Big\|\frac{1}{C_3S})+L_1S+\frac{1}{C_1S} \\ \\ Z_{21}=\frac{V_2}{I_1}\Big|_{I_2=0}=R_2\times\frac{R_1}{R_1+Y}\times\dfrac{L_3S\Big\|\frac{1}{C_3S}}{L_3S\Big\|\frac{1}{C_3S}+\frac{1}{C_2S}+L_2S+R_2} \end{cases} \tag{7}$$

$$z_{22} = \frac{V_2}{I_2}\Big|_{I_1=0} = \tag{8}$$
$$\left[\left(R_1+\frac{1}{C_1+S}+L_1S\right)\Big\|(L_3S\Big\|\frac{1}{C_3S})+\frac{1}{C_1S}+L_2S\right]\|R_2$$

$$S_{11} = \frac{(Z_{11}-Z_0)(Z_{22}+Z_0)-Z_{12}Z_{21}}{(Z_{11}+Z_0)(Z_{22}+Z_0)-Z_{12}Z_{21}}, \tag{9}$$

$$S_{21} = \frac{2Z_{21}Z_0}{(Z_{11}+Z_0)(Z_{22}+Z_0)-Z_{12}Z_{21}}. \tag{10}$$

Figures 6 and 7 show the simulated reflection waveforms observed at Port1 of the defected structures, as shown in Fig. 2, and with a 50 Ω termination on Port2, before and after optimization, respectively. The excitation source is a step wave with amplitude 1Volt and rise time of 30psec. The corresponding result

predicted by the equivalent circuit model is also shown in these figures. As shown in Figs. 6 and 7, TDR curves have started with impedance just under 50 Ω. This is indeed the characteristic impedance of the microstrip line. At impedance discontinuities, part of the input signal is reflected. These reflections, after traveling back, reach terminal Port1 and are observed there [22-23].
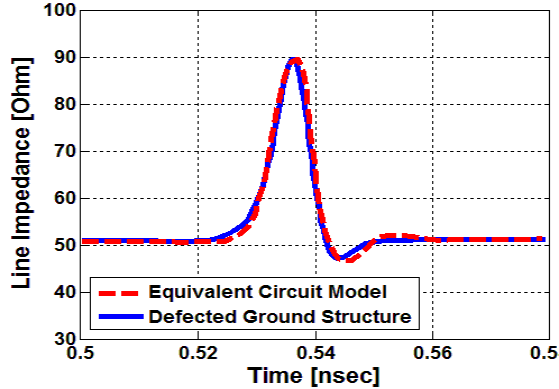

Fig. 6. The reflected waveforms simulated by HFSS and predicted by equivalent circuit model the proposed defected microstrip structure shown in Fig. 2 before optimization.
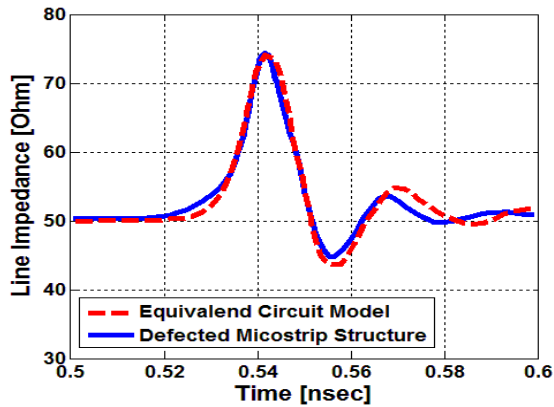

Fig. 7. The reflected waveforms simulated by HFSS and predicted by equivalent circuit model the proposed defected ground structure shown in Fig. 2 after optimization by GA.

From these observations, the characteristic impedances along the transmission line can be computed. From these formulas, the characteristic impedances along the transmission line can be computed. The optimal dimensions of the equivalent circuit models parameters calculated from ordinary TDR and modified TDR by genetic algorithm technique are specified in Table 2.

Table 2: The equivalent circuit models parameters calculated from ordinary TDR and modified TDR by genetic algorithm technique

Element	Before Optimization	After Optimization
L_1	1.55 (nH)	1.61 (nH)
C_1	1.05 (pF)	1.15 (pF)
R_1	0.8 (Ω)	0.76 (Ω)
L_2	4.8 (nH)	4.6 (nH)
C_2	1.75 (pF)	1.7 (pF)
R_2	2.1 (Ω)	2.05 (Ω)

III. RESULTS AND DISCUSSIONS

The proposed microstrip-fed slot antenna with various design parameters were constructed, and the numerical and experimental results of the input impedance and radiation characteristics are presented and discussed.

The configuration of the presented slot antenna was shown in Fig. 1. Geometry for the ordinary slot antenna (Fig. 8 (a)), with two inverted U-shaped slots in the ground plane (Fig. 8 (b)), and the proposed antenna (Fig. 8 (c)) structures are shown in Fig. 8. VSWR characteristics for the structures that were shown in Fig. 6 are compared in Fig. 9. As shown in Fig. 9, it is observed that the upper frequency bandwidth is affected by using the pair of inverted U-shaped slots in the ground plane and notched frequency bandwidth is sensitive to the M-shaped SIR slot.

To understand the phenomenon behind the bandwidth enhancement performance, simulated current distributions for the proposed antenna on the ground plane at 12 GHz is presented in Fig. 10 (a). It is found that by using two inverted U-shaped slots, an additional current path in the ground plane is generated and a new resonance at 12 GHz can be achieved. Another important design parameter of this structure is the M-shaped slot at the feed-line. Figure 10 (b) presents the simulated current distributions on the radiating stub and feed-line at the notched frequency (7.5 GHz). As shown in Fig. 10 (b), at the notched frequency the current flows are more dominant around of the M-shaped slot at feed-line.
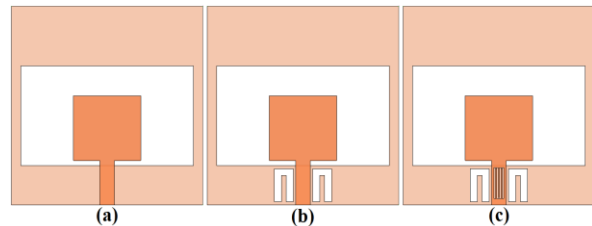

Fig. 8. (a) Ordinary slot antenna, (b) the antenna with a pair of inverted U-shaped slots, and (c) the proposed antenna.
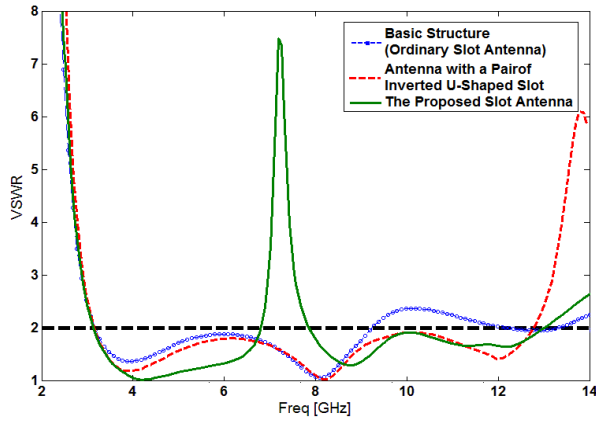
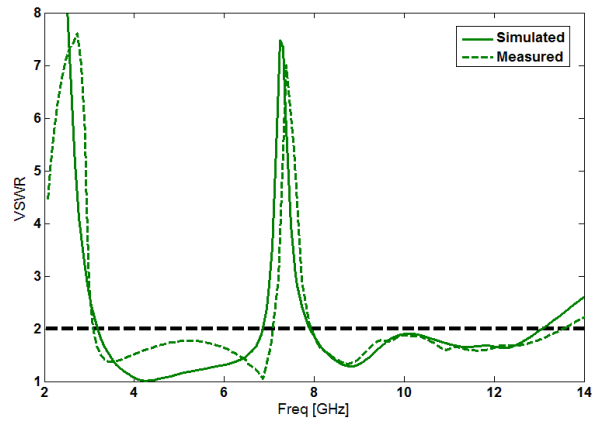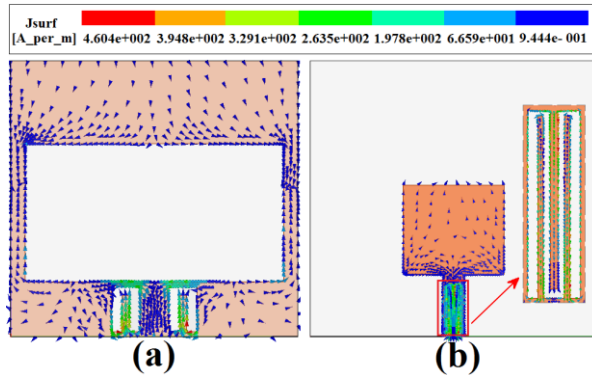Fig. 9. Simulated VSWR characteristics for antennas shown in Fig. 6.

Fig. 10. Simulated surface current distributions for the proposed antenna: (a) on the ground at 12 GHz (new resonance frequency), and (b) on the square radiating stun and feed-line at 7.5 GHz (notched frequency).

The proposed antenna with final design was built and tested. The measured and simulated VSWR characteristics of the proposed antenna were shown in Fig. 11. Fabricated antenna has the frequency band of 3.03 to 13.21 GHz with a band-notched performance around 7.22 to 7.81 GHz.

Figure 12 shows the measured radiation patterns including the co-polarization in the H-plane (x-z plane) and E-plane (y-z plane). The main purpose of the radiation patterns is to demonstrate that the antenna actually radiates over a wide frequency band. It can be seen that the radiation patterns in *x-z* plane are nearly omnidirectional for the three frequencies. The radiation patterns on the y-z plane are like a small electric dipole leading to bidirectional patterns in a very wide frequency band [24-25].
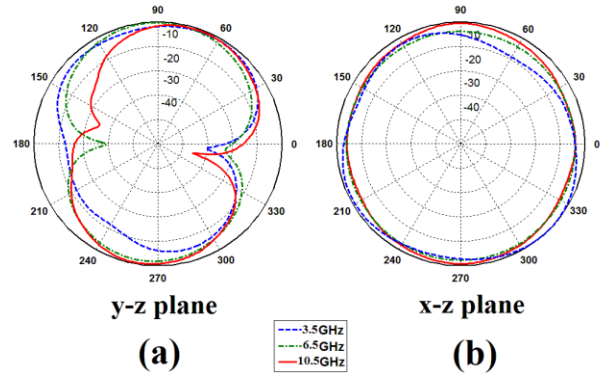

Fig. 11. Measured and simulated VSWR characteristics for the proposed antenna.

Fig. 12. Measured radiation patterns of the proposed antenna: (a) E-plane and (b) H-plane.

IV. CONCLUSION

In this paper, a novel band-notched slot antenna with a time domain method to extract the equivalent RLC of the defected structures for UWB applications has been proposed. The analytic formulations for the equivalent circuit models are obtained based on time-domain reflectometry theory. Furthermore, using Genetic Algorithm Optimization, the accuracy of the equivalent circuit models of the employed DGS and DMS have been improved significantly. The fabricated antenna covers the frequency range for UWB systems between 3.03 to 13.21 GHz with a band-notched characteristic in the frequency range of 7.25 to 7.75 GHz to avoid interference from X-band communication systems. The proposed band-notched UWB antenna has compact and simple configuration and is easy to fabricate. Experimental results show that the proposed antenna could be a good candidate for UWB applications.

REFERENCES

[1] H. Schantz, *The Art and Science of Ultra Wideband Antennas*. Artech House, 2005.

[2] A. Dastranj and H. Abiri, "Bandwidth enhancement of printed E-shaped slot antennas fed by CPW and microstrip line," *IEEE Trans. Antenna Propag.*, vol. 58, pp. 1402-1407, 2010.

[3] Y. W. Jang, "Experimental study of large bandwidth three-offset microstrip line-fed slot antenna," *IEEE Microw. Wireless Comp. Lett.*, vol. 11, pp. 425-426, 2001.

[4] N. Ojaroudi, "Bandwidth improvement of monopole antenna using π-shaped slot and conductor-backed plane," *International Journal of Wireless Communications, Networking and Mobile Computing*, vol. 1, pp. 14-19, 2014.

[5] N. Ojaroudi, "Compact UWB monopole antenna with enhanced bandwidth using rotated L-shaped slots and parasitic structures," *Microw. Opt. Technol. Lett.*, vol. 56, pp. 175-178, 2014.

[6] M. K. Kim, Y. H. Suh, and I. Park, "A T-shaped microstrip line-fed wide-slot antenna," *in Proc. IEEE AP-S Int. Symp.*, pp. 1500-1503, 2000.

[7] K. Chung, T. Yun, and J. Choi, "Wideband CPW fed monopole antenna with parasitic elements and slots," *Electronics Letters*, vol. 40, no. 17, pp. 1038-1040, 2004.

[8] N. Ojaroudi and M. Ojaroudi, "Novel design of dual band-notched monopole antenna with bandwidth enhancement for UWB applications," *IEEE Antennas Wireless Propag. Lett.*, vol. 12, pp. 698-701, 2013.

[9] N. Ojaroudi, M. Ojaroudi, and N. Ghadimi, "UWB monopole antenna with WLAN frequency band-notched performance by using a pair of E-shaped slits," *Applied Computational Electromagnetics Society (ACES) Journal*, vol. 28, pp. 1244-1249, 2014.

[10] N. Ojaroudi, "A modified compact microstrip-fed slot antenna with desired WLAN band-notched characteristic," *American Journal of Computation, Communication and Control*, vol. 1, pp. 56-60, 2014.

[11] N. Ojaroudi, "Application of protruded strip resonators to design an UWB slot antenna with WLAN band-notched characteristic," *Progress in Electromagnetics Research C*, vol. 47, pp. 111-117, 2014.

[12] N. Ojaroudi and M. Ojaroudi, "Dual band-notched monopole antenna with multi-resonance characteristic for UWB wireless communications," *Progress in Electromagnetics Research C*, vol. 40, pp. 188-199, 2013.

[13] N. Ojaroudi and M. Ojaroudi, "A novel design of reconfigurable small monopole antenna with switchable band notch and multi-resonance functions for UWB applications," *Microw. Opt. Technol. Lett.*, vol. 55, pp. 652-656, 2013.

[14] N. Ojaroudi, M. Mehranpour, S. Ojaroudi, and Y. Ojaroudi, "Application of the protruded structures to design an UWB slot antenna with band-notched characteristic," *Applied Computational Electromagnetics Society (ACES) Journal*, vol. 29, pp. 184-189, 2014.

[15] N. Ojaroudi, "Application of protruded Γ-shaped strips at the feed-line of UWB microstrip antenna to create dual notched bands," *International Journal of Wireless Communications, Networking and Mobile Computing*, vol. 1, pp. 8-13, 2014.

[16] N. Ojaroudi and M. Ojaroudi, "An UWB slot antenna with band-stop notch," *IET Microw. Antennas Propag.*, vol. 10. pp. 831-835, 2013.

[17] A. B. Abdel-Rahman, A. K. Verma, A. Boutejdar, and A. S. Omar, "Control of bandstop response of Hi-Lo microstrip low-pass filter using slot in ground plane," *IEEE Trans. Microw. Theory Tech.*, vol. 52, pp. 1008-1013, Mar. 2004.

[18] C.-S. Kim, J.-S Lim, J.-H. Kim, and D. Ahn, "A design of a miniaturized 2-pole bandpass filter by using slot and hair-pin line," *in IEEE MTT-S Int. Dig.*, Fort Worth, TX, pp. 1983-1986, June 2006.

[19] C. H. Cheng, C. H. Tsai, and T. L. Wu, "A novel time domain method to extract equivalent circuit model of patterned ground structures," *IEEE Microw. Wireless Compon. Lett.*, vol. 17, pp. 486-488, 2010.

[20] X. Zeng, J. He, M. Wang, and M. Abdulla, "New closed-form formula for series inductance and shunt capacitance based on measured TDR impedance profile," *IEEE Microw. Wireless Compon. Lett.*, vol. 17, pp. 781-783, 2007.

[21] Ansoft High Frequency Structure Simulator (HFSS), ver. 13, Ansoft Corporation, 2011.

[22] A. J. Kerkhoff, R. L. Rogers, and H. Ling, "Design and analysis of planar monopole antennas using a genetic algorithm approach," *IEEE Trans. Antennas Propag.*, vol. 2, pp. 1768-1771, 2004.

[23] A. J. Kerkhoff and H. Ling, "Design of a band-notched planar monopole antenna using genetic algorithm optimization," *IEEE Trans. Antennas Propag.*, vol. 55, pp. 604-610, 2007.

[24] N. Ojaroudi and M. Ojaroudi, "Dual band-notched monopole antenna with multi-resonance characteristic for UWB wireless communications," *Progress in Electromagnetics Research C*, vol. 40, pp. 188-199, 2013.

[25] N. Ojaroudi, S. Amiri, F. Geran, and M. Ojaroudi,

"Band-notched small monopole antenna using triple E-shaped structures for UWB systems," *Applied Computational Electromagnetics Society (ACES) Journal*, vol. 27, no. 12, pp. 1022-1028, 2012.